International Journal of Biological Macromolecules 114 (2018) 373–380

Contents lists available at ScienceDirect

International Journal of Biological Macromolecules

journal homepage: http://www.elsevier.com/locate/ijbiomac

Preparation, characterization, and biodegradation of poly(butylene succinate)/cellulose triacetate blends

Ke Shi [a,1], Yun Liu [b,1], Xueyan Hu [c], Tingting Su [a,*], Ping Li [a], Zhanyong Wang [a,*]

[a] College of Chemistry, Chemical Engineering and Environmental Engineering, Liaoning Shihua University, Fushun 113001, China
[b] College of Life Sciences and Oceanography, Shenzhen University, Shenzhen 518060, China
[c] State Key Laboratory of Fine Chemicals, Dalian R&D Center for Stem Cell and Tissue Engineering, Dalian University of Technology, Dalian 116024, China

ARTICLE INFO

Article history:
Received 21 January 2018
Received in revised form 22 March 2018
Accepted 24 March 2018
Available online 27 March 2018

Keywords:
Poly(butylene succinate)
Cellulose triacetate
Blend

ABSTRACT

Poly(butylene succinate) (PBS) and cellulose triacetate (CT) were blended using chloroform as solvent. The solid-state properties of PBS/CT blends were confirmed by Fourier transform infrared spectroscopy (FTIR), differential scanning calorimetry (DSC), X-ray diffraction (XRD), thermogravimetric analysis, scanning electron microscopy (SEM), and water contact angle measurements. FTIR results show that PBS and CT were physically blended. Tensile strength was not distinguished when the weight percent of CT was <15%, and Young's modulus increased gradually with increasing CT. DSC and XRD results show that the crystals were homogeneous, and crystallinity had no apparent decrease when <10% CT was added to the PBS matrix. However, the addition of more CT components could destroy the crystal behavior of PBS. SEM showed that no phase separation occurred between the two materials. The addition of CT increased the hydrophilicity of PBS/CT1–15 blends. The weight loss was nearly 90% after 16 h of degradation for PBS/CT10. The appropriate proportion of PBS to CT was 90:10.

1. Introduction

Poly(butylene succinate) (PBS) has attracted much interest as one of the biodegradable polymers on academic and industrial territories [1]. PBS has many excellent characteristics, including low cost, well processability, robust thermal stability, and chemical resistance [2–5]. Therefore, PBS is usually used in toys, food packaging, disposable tableware, and biomedical fields [6–9].

Cellulose and its derivatives are usually used to modify PBS-based polymer as one of the most abundant renewable materials [10]. PBS [11], polylactic acid [12], poly(butylene succinateco-butylene adipate) [13], and poly(butyleneadipate-co-terephthalate) [14] have been modified using cellulose and its derivatives. The composites have appealing properties after blending, including excellent mechanical properties, high aspect ratio, high surface area, good thermal resistance, free from harm, low energy consumption [15], and appropriate hydrophilic properties [16–20].

However, the major restraints to the properties of compositions are poor compatibility and interfacial adhesion between polymer and cellulose. Therefore, cellulose is always functionalized with other materials before using.

Cellulose triacetate (CT) is obtained by converting all hydroxyl groups to acetyl groups, which can enhance solubility in organic solvents and heat resistance [21,22]. CT has relatively high hydrophilicity, wide availability, good mechanical strength, and certain resistance to chlorine and other oxidants [23,24].

PBS/cellulose acetate, PBS/cellulose diacetate, and PBS/CT blends had been prepared and their structure and physical properties had been investigated [25–28]. Číhal et al. prepared PBS/CT blends containing 0–50 wt% of PBS and discussed the influence of the PBS content on the physical structure and thermal properties of the CT-rich blends [28]. In this study, PBS was modified with CT through melt blending. Some solid-state properties, including crystallization behavior, thermal stability, mechanical properties, and hydrophilic properties of the blends, were studied. The biodegradation behavior of PBS/CT blends was also investigated using the mixture of cutinase and cellulase.

2. Materials and methods

2.1. Materials

PBS was obtained from Anqing He Xing Chemical Corp. Ltd., China with number average molecular weight from 150,000 g/mol to

* Corresponding authors.
E-mail addresses: sutingting1978@126.com (T. Su), wangzy125@gmail.com (Z. Wang).
[1] Ke Shi and Yun Liu equally contributed to this work.

https://doi.org/10.1016/j.ijbiomac.2018.03.151
0141-8130/

210,000 g/mol. CT was obtained from Acros Organics (code number: 177822500), USA. Cutinase was purified from the zymotic fluid of recombinant *Pichia pastoris* containing a gene encoding cutinase from *Fusarium solani* [29]. Cellulase R-10 derived from *Trichoderma viride* was purchased from Yakult Pharmaceutical Industry Co., Ltd. (Japan). All of the chemicals were analytical grade reagents.

2.2. Synthesization of PBS/CT composites via melt blending

PBS and CT powders were dried in a vacuum at 50 °C for 8 h. They were mixed with ratios of 99/1, 95/5, 90/10, 85/15, 80/20, 75/25, and 70/30 in chloroform at 65 °C under condensing and stirring for 120 min. Neat PBS was processed under the same conditions. The obtained blends films (thickness of 0.5 mm) were hot-pressed at 160 °C and cold-pressed at 30 °C. Subsequently, dry the blends for 48 h in a fume hood and for 24 h in vacuum at 50 °C to remove chloroform. PBS/CT blends were named PBS/CT1–PBS/CT30, which corresponded to the weight fractions of 99/1–70/30, respectively.

2.3. Fourier transform infrared spectroscopy (FTIR)

ATR-FTIR analysis was carried out at an Agilent Cary 660 FTIR spectrometer (USA) with a resolution of 2 cm^{-1}. The wavenumber was from 4000 cm^{-1} to 400 cm^{-1} with 18 scan times.

2.4. Scanning electron microscopy (SEM)

The surface of the blends was observed using field emission SU8010 SEM (Japan) at an acceleration voltage of 5 kV. A thin gold layer was coated on the surface of the film prior to testing.

2.5. Differential scanning calorimetry (DSC)

The DSC experimental was performed using TA Q20 (USA) in nitrogen. Samples were heated from 40 °C to 150 °C at a rate of 10 °C/min, held for 5 min, and then cooling down to 40 °C at the same rate. The samples were scanned again at the same condition. The crystallinity (X_c) was calculated using Eq. (1):

$$X_c = \frac{\Delta H_m}{f_p \times \Delta H_m^0} \times 100\%, \quad (1)$$

where ΔH_m = the melting enthalpy, J/g), f_p = the mass fraction of PBS, and ΔH_m^0 = 110.3 J/g (the melting enthalpy of 100% crystallinity PBS) [30].

2.6. X-ray diffraction (XRD)

XRD experiments were completed on a Bruker D8 Advance XRD (Germany) employing a Cu Kα radiation. The acceleration voltage is 40 kV with 200 mA. The diffraction angles were from 5° to 50° at a scan rate of 5° min^{-1}.

2.7. Mechanical properties

Mechanical properties of the samples were finished by an Instron (Canton, MA) 5500R Universal Testing Machine (USA) with a crosshead speed of 10 mm/min. All films were cut into 60 mm × 25 mm × 0.5 mm in length, width, and thickness, respectively.

2.8. Thermal stability analysis

Thermogravimetric (TG) analysis of the samples was conducted using a Q600 TG analyzer (TA, USA). Heating was performed from 30 °C to 500 °C at a heating rate of 20 °C/min in nitrogen.

2.9. Water contact angle (WCA)

The hydrophilic properties were determined by WCA measurements (DSA100, KRUSS, Germany). The water was injected at a speed of 0.6 μL s^{-1}. All samples were measured five times at the round and center of every film. The final value was the average of the five numbers.

2.10. Enzymatic degradation

The blend films, 30 mm × 10 mm × 0.5 mm in length, width, and thickness, were incubated in K_2HPO_4/KH_2PO_4 buffer (0.1 M, pH 7.2) containing 0.15 U/mL cutinase and 0.2 U/mL cellulase at 45 °C. Collect the degraded films, wash with deionized water after incubating, and dry the cleaned films at 50 °C in vacuum. The weight loss rate before and after degradation was calculated according to Eq. (2):

$$W_{loss}(\%) = \frac{W_{before} - W_{after}}{W_{before}} \times 100\%, \quad (2)$$

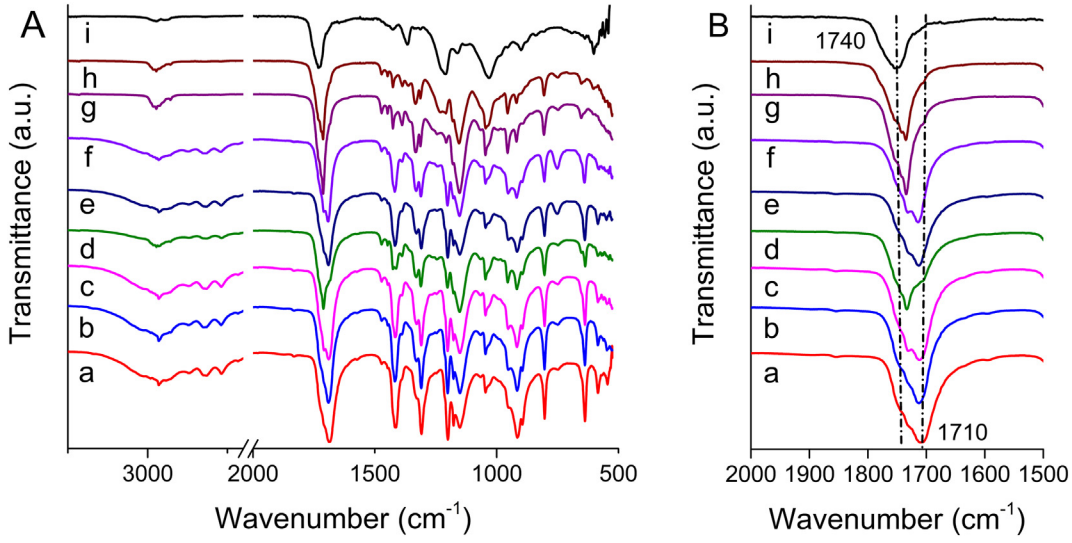

Fig. 1. FTIR spectra of (a) neat PBS, (b) PBS/CT1, (c) PBS/CT5, (d) PBS/CT10, (e) PBS/CT15, (f) PBS/CT20, (g) PBS/CT25, (h) PBS/CT30, and (i) neat CT. Spectra (A) is from 3500 cm^{-1} to 500 cm^{-1}, and (B) is from 2000 cm^{-1} to 1500 cm^{-1}.

where W_{loss} (%) = the weight loss rate. W_{before} and W_{after} were the weight of the film before and after degradation, respectively.

3. Results and discussion

3.1. ATR-FTIR analysis of PBS/CT

The FTIR spectra of neat PBS, neat CT, and their blends in the region from 3500 to 500 cm^{-1} and 2000 to 1500 cm^{-1} are shown in Fig. 1. For the neat PBS, the C═O stretching vibration was located at 1710 cm^{-1}. The band of neat PBS at 1046 cm^{-1} was due to ν_{C-O}. The peak of neat PBS at 1155 cm^{-1} was assigned to the $\nu_{-C-O-C-}$ [31]. For the neat CT, the main characteristic peaks at 1740, 1366, 1214, and 1031 cm^{-1} were due to the stretching vibration of C═O and C—O in CT structure [32,33]. The main absorption bands of PBS/CT blends were the overlap of neat PBS and CT, which indicated that no reaction occurred between the two components. However, a small but distinctive difference can be found between the spectra of the pure components and blends (see Fig. 1(B)). In the carbonyl-stretching region, the band of neat PBS is located at 1710 cm^{-1}. It is shifted to higher wavenumber below 1740 cm^{-1} in the complexes (Fig. 1b–h). This change may be the result of the inhibition of crystallization of PBS chains in the complexes [27,34] (see Section 3.4). The split peaks of PBS/CT blends are the overlapping of the single peaks of neat PBS and CT in the carbonyl-stretching region.

3.2. Fracture morphologies of composites

The micrographs of the fracture surfaces of PBS/CT composites are illustrated in Fig. 2. The surface of the blends was flattened because PBS and CT were compatible materials. CT powders were evenly dispersed in the PBS matrix. The cross section of the PBS/CT1 (Fig. 2a) was relatively smooth after the brittle cold treatment of liquid nitrogen. The

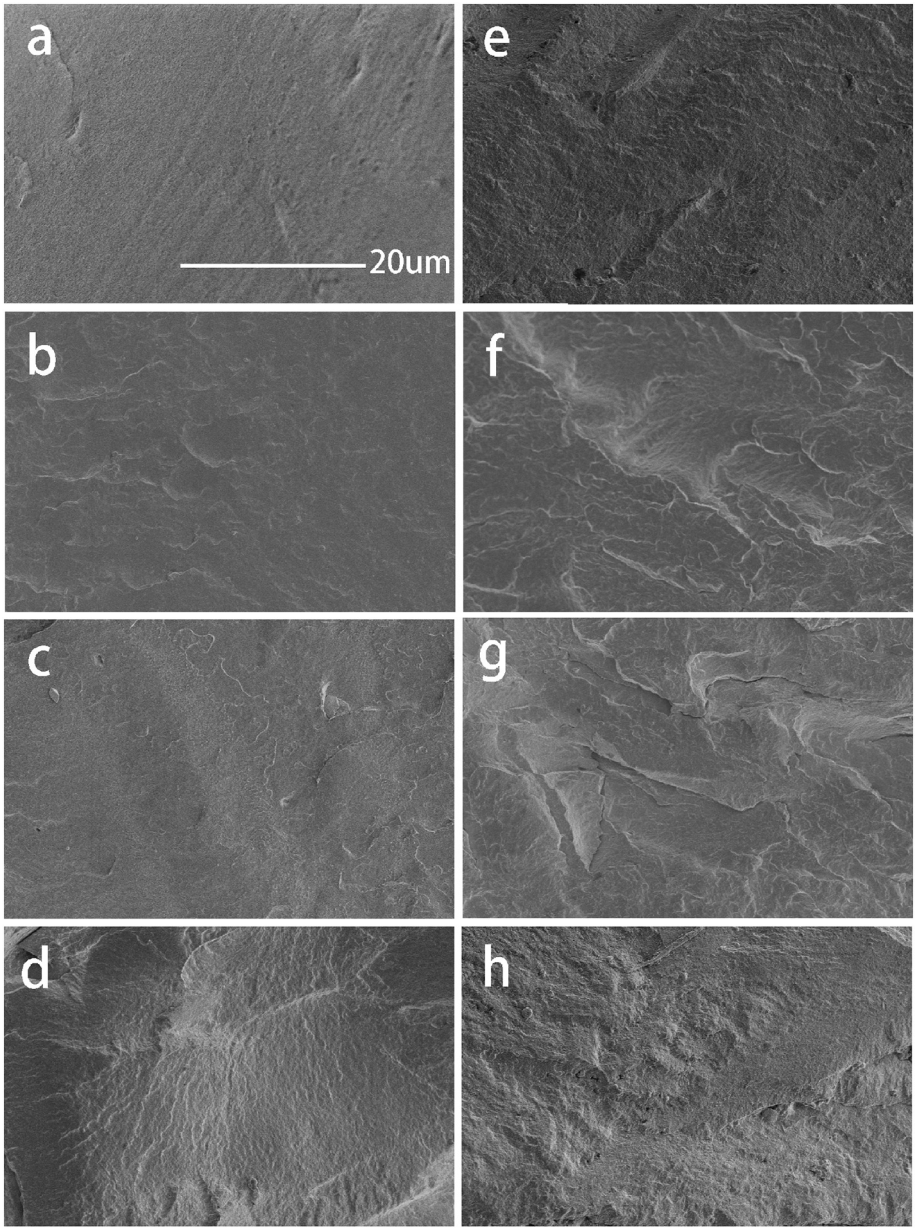

Fig. 2. SEM of fractured surface of (a) neat PBS, (b) PBS/CT1, (c) PBS/CT5, (d) PBS/CT10, (e) PBS/CT15, (f) PBS/CT20, (g) PBS/CT25, and (h) PBS/CT30.

cross section had no clear difference between neat PBS and PBS/CT blends when 1%–10% of CT was added to the PBS matrix (Fig. 2b–d). The cross section became increasingly rough when >15% CT was added in the PBS matrix. These results indicate that the mechanical properties may be poor for PBS/CT15–30 blends.

3.3. Mechanical properties

The mechanical properties of PBS/CT blends are illustrated in Fig. 3. The tensile strength was not apparent when the weight percent of CT was <15%. However, it decreased dramatically for PBS/CT25 and PBS/CT30 blends. The elongation at break clearly decreased with the increase in CT. Meanwhile, the Young's modulus of the PBS composite increased gradually with increasing CT. Young's modulus values sharply increased to 41% and 67% for PBS/CT10 and PBS/CT15 compositions, respectively. An enhancement of the rigidity of the blends was indicated. Literature [35] had reported a similar result, and they claimed the tensile modulus increased to about 50% by incorporating kenaf fiber to PBS directly. In general, the relationship between the matrix and filler, including dispersion, interfacial interaction, lamellar thickness, crystallinity, and orientation can all influence the mechanical property of the blends [35]. However, the tensile strength and elongation at break did not as high as what we expected. They could be improved only when the dispersion, adhesion, and crystallinity were enhanced simultaneously, such as treating cellulose with chloride [36], adding certain compatibilizer [37,38], or modifying matrix with peroxide [13].

3.4. Crystalline properties

The crystalline parameters of PBS/CT compositions are displayed in Fig. 4 and Table 1. In Fig. 4a, the crystallization peaks of PBS/CT samples were flatter and blunter for PBS/CT15–30 compared with that of neat PBS. Thus, the crystals were possibly not homogeneous when above 15% CT was added in the PBS matrix, which indicated that the uniformity of PBS was destroyed by the more CT components. This observation may be due to crystallization being dependent on the concentration and mobility of PBS molecular chains in the blend. The large CT molecule restricts the growth of PBS crystallites and results in the decrease in T_c. Therefore, the composites are difficult to complete crystallization with high amounts of CT filler.

As shown in Fig. 4b, for neat PBS an endothermic peak at 104.65 °C and an exothermic peak at 86.00 °C appeared [39]. The distinction in T_m was not apparent when the addition of CT was <10%. Similar results were found in the literature [37]. T_m of PBS/CT blends clearly decreased for PBS/CT15–30. The decrease in T_m and ΔH_m indicated that a high amount of CT restricted the molecule to mobile and hindered to crystallize. As the two components did not react, crystallization could not occur freely. Therefore, the tendency to crystallize for PBS/CT segments was constrained, which resulted in low crystallinity. Similar observations were reported by Leandro et al. [40].

The XRD results of PBS/CT blends were investigated, as shown in Fig. 5. The diffraction peaks of PBS were observed at 19.5°, 21.5°, and 22.5°, respectively [13]. CT did not exhibit diffraction peaks, which indicated that CT was mainly formed by the amorphous form of polymerization. The PBS/CT blends showed diffraction peaks close to those of PBS, but the intensity of the diffraction peaks weakened with the increase in CT amount. This finding suggested that the crystallinity of the blend decreased. Furthermore, the presence of CT did not promote the crystallization of PBS but restricted the movement of PBS molecules. This result agreed with the DSC results (Table 1).

3.5. Thermal properties

The thermal degradation behaviors of PBS/CT blends are listed in Fig. 6 and Table 2. $T_{-5\%}$ and $T_{-50\%}$ are the temperatures at 5% and 50% degradation, respectively. T_{max} is the maximum decomposition temperature. All samples followed one-step weight loss. The thermal stability slightly increased when the amount of addition was <10%. Moreover, it dropped to less for PBS/CT15 to PBS/CT30.

3.6. Hydrophilicity

Hydrophilicity can be deduced from the static contact angle of the polymer film. During the hydrophilicity test (Fig. 7), hydrophilicity initially increased and then decreased with the increase in CT. CT has relatively high hydrophilicity [23]. Thus, the hydrophilic properties of CT increased the hydrophilicity of PBS blends. When PBS/CT was 95/5, the WCA was the lowest, which indicated that the presence of CT increased the hydrophilicity of PBS-modified materials. However, the

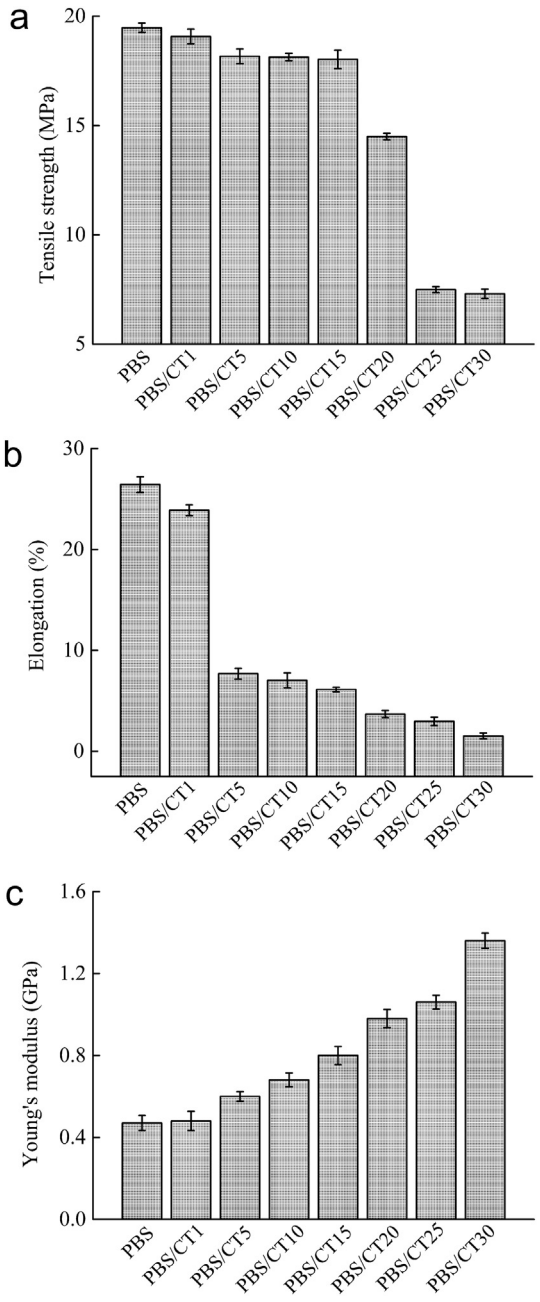

Fig. 3. (a) Tensile strength, (b) elongation at break, and (c) Young's modulus of PBS/CT blends.

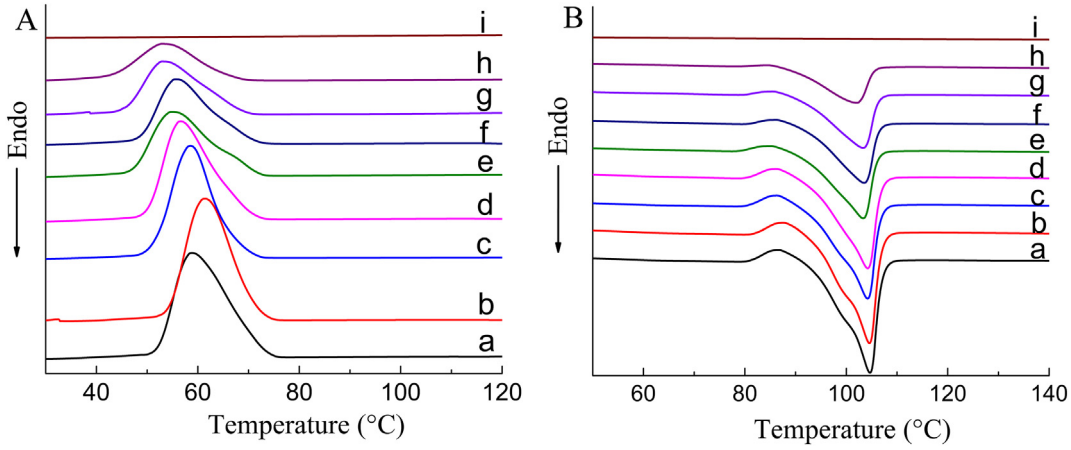

Fig. 4. DSC curves of (a) neat PBS, (b) PBS/CT1, (c) PBS/CT5, (d) PBS/CT10, (e) PBS/CT15, (f) PBS/CT20, (g) PBS/CT25, (h) PBS/CT30, and (i) neat CT on the (A) first cooling run and (B) second heating run.

Table 1
Thermal properties of neat PBS and PBS/CT blends.

Sample	First cooling run		Second heating run		
	T_c (°C)	ΔH_c (J/g)	T_m (°C)	ΔH_m (J/g)	X_c (%)
PBS	58.9	56.0	104.7	67.4	61.1
PBS/CT1	61.4	56.1	104.6	65.3	59.8
PBS/CT5	59.2	49.7	104.2	59.2	56.5
PBS/CT10	56.7	48.7	104.2	57.4	57.8
PBS/CT15	54.2	39.1	103.3	45.4	48.5
PBS/CT20	55.8	38.0	103.5	43.3	49.0
PBS/CT25	53.1	32.5	103.3	39.3	47.5
PBS/CT30	53.1	23.3	102.0	28.1	36.3

hydrophilicity of these films had no significant difference with neat PBS when the CT content was above 20%.

3.7. Enzymatic degradability

Fig. 8 presents the weight loss of PBS/CT films degraded in the mixture of cutinase and cellulase. The weight loss of the blends showed an increasing trend with prolonged degradation time. The enzymatic degradation of neat PBS was rapid, which was completed after approximately 12 h [29]. The low-molecular-weight fragments and exposed end groups in PBS degraded rapidly at the initial stage [41]. The weight loss of the PBS/CT blends was lower at varying degrees compared with that of neat PBS. The similar trend was reported [42,43]. Slow biodegradation is due to the increase in the barrier properties after blending with other components, which restrict the penetration of enzymes through materials. In general, the dispersion and distribution of cellulose in the polymer matrix could become the barrier of polymer composites. Based on our previous publication, poor dispersion of cellulose microcrystalline and cellulose acetate in PBS matrix indicated high weight loss [44]. This finding indicated that the rich filling dispersed in the PBS matrix possibly increased the barrier, which could lead to low biodegradation. However, the weight loss was nearly 90% after 16 h of degradation for PBS/CT10.

The SEM results of PBS/CT blends degraded for 4 h are shown in Fig. 9. In Fig. 9a, the surfaces of the degraded PBS were rough, and most showed a spherulitic texture. The impinging lines were degraded first, followed by the other parts. The surfaces for the PBS/CT blends (Fig. 9b–h) were different with neat PBS (Fig. 9a). In PBS/CT samples, most degraded surfaces were smooth. The particles of PBS matrix and CT filler

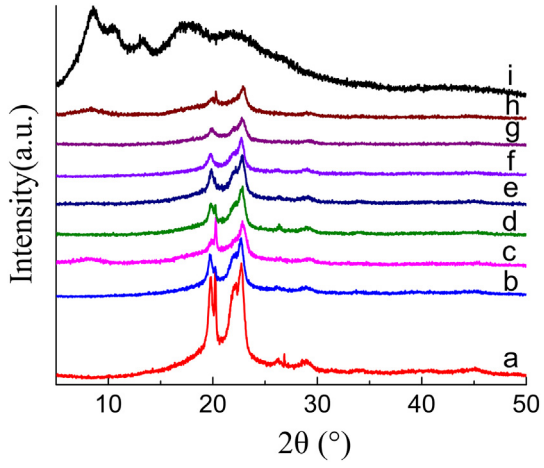

Fig. 5. XRD of (a) neat PBS, (b) PBS/CT1, (c) PBS/CT5, (d) PBS/CT10, (e) PBS/CT15, (f) PBS/CT20, (g) PBS/CT25, (h) PBS/CT30, and (i) neat CT.

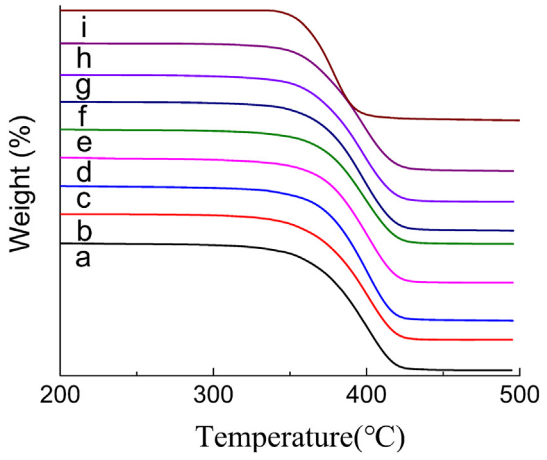

Fig. 6. TG curves of (a) neat PBS, (b) PBS/CT1, (c) PBS/CT5, (d) PBS/CT10, (e) PBS/CT15, (f) PBS/CT20, (g) PBS/CT25, (h) PBS/CT30, and (i) neat CT.

Table 2
Thermal stability of neat PBS and composites.

	PBS	PBS/CT1	PBS/CT5	PBS/CT10	PBS/CT15	PBS/CT20	PBS/CT25	PBS/CT30
$T_{-5\%}$	339.1	342.4	340.8	339.0	337.6	337.6	337.5	338.3
$T_{-50\%}$	393.9	395.3	395.9	396.4	397.8	393.6	392.3	391.2
T_{max}	396.3	400.4	400.9	400.7	397.7	396.8	397.0	396.7

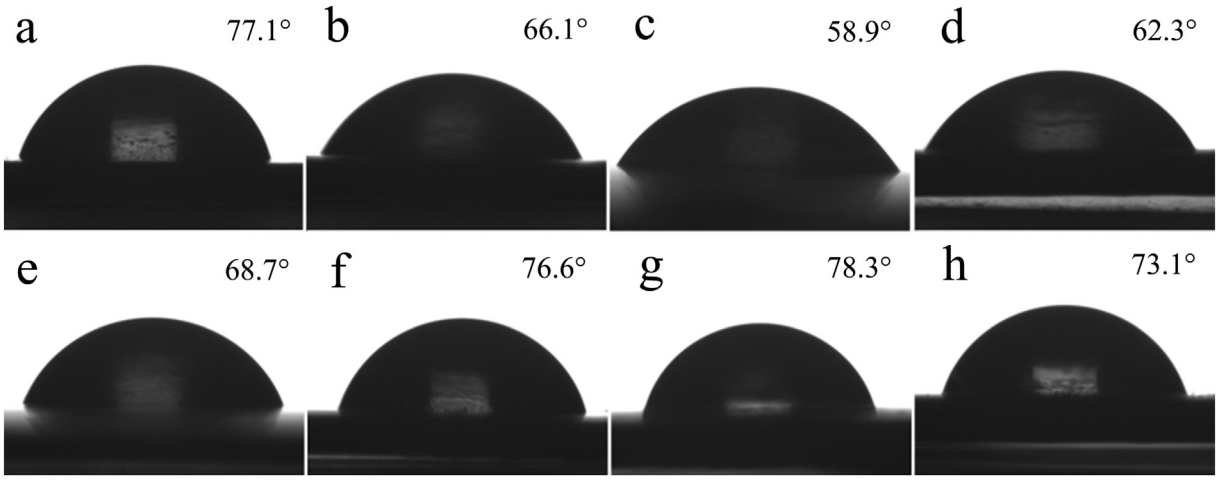

Fig. 7. WCA of composites: (a) neat PBS, (b) PBS/CT1, (c) PBS/CT5, (d) PBS/CT10, (e) PBS/CT15, (f) PBS/CT20, (g) PBS/CT25, and (h) PBS/CT30.

were packed densely because they dispersed uniformly (Fig. 2b–h). Therefore, the enzyme molecules did not easily enter the blend bulk. It means that the degradation occurred only on the surface of the blends (Fig. 9b–h). Similar result has been reported in our previous study [44]. Although low crystallization and hydrophilicity both contribute to the biodegradation of polymer [45,46], the weight loss sharply decreased when large amount CT were added in the PBS matrix.

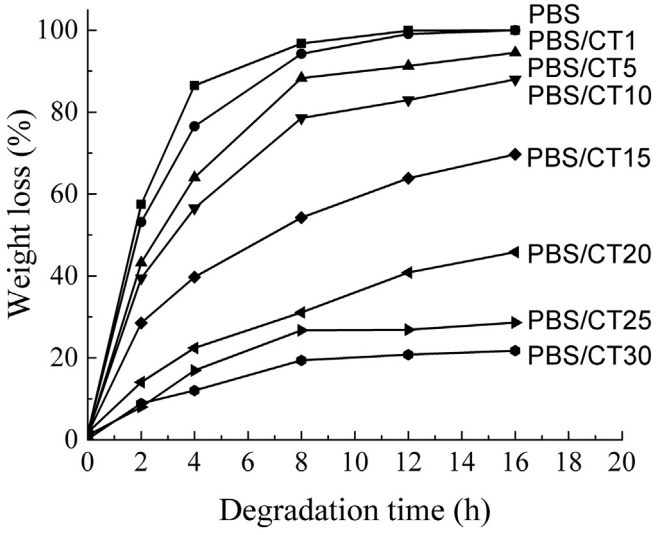

Fig. 8. Weight loss of PBS/CT films with different contents of CT degraded by the mixture of cutinase and cellulase after varying degradation periods.

4. Conclusions

PBS and CT were blended with different ratios using chloroform as a solvent. As confirmed by the analysis of mechanical properties, the Young's modulus of PBS/CT composites increased from 47.47 MPa to 136.32 MPa with increasing CT content from 0% to 30%. The results of DSC and XRD showed that less amount of CT (<10%) added to PBS did not change the crystal behavior. However, X_c and T_c of blend films exhibited a downward trend when the content of CT exceeded 15%. Thermal stability only slightly increased when the amount of addition was <10%. When PBS/CT was <10%, the WCA was lower than that of neat PBS. This finding indicated good hydrophilicity. The weight loss and morphological analysis of PBS/CT composites before and after degradation by the cutinase and cellulose mixture showed that CT addition decreased the degradability of PBS. However, the weight loss became close to 90% after 16 h of degradation for PBS/CT10. Therefore, the blend economized the PBS material, was environment friendly, and showed preferable solid-state properties when the amount of CT was 10%.

Acknowledgement

This work was supported by National Natural Science Foundation of China (Grant No. 31570097), Science Project of Liaoning Province Education Office (Grant No. L2016002) and the Program for Liaoning Innovative Talents in University (LR2017063).

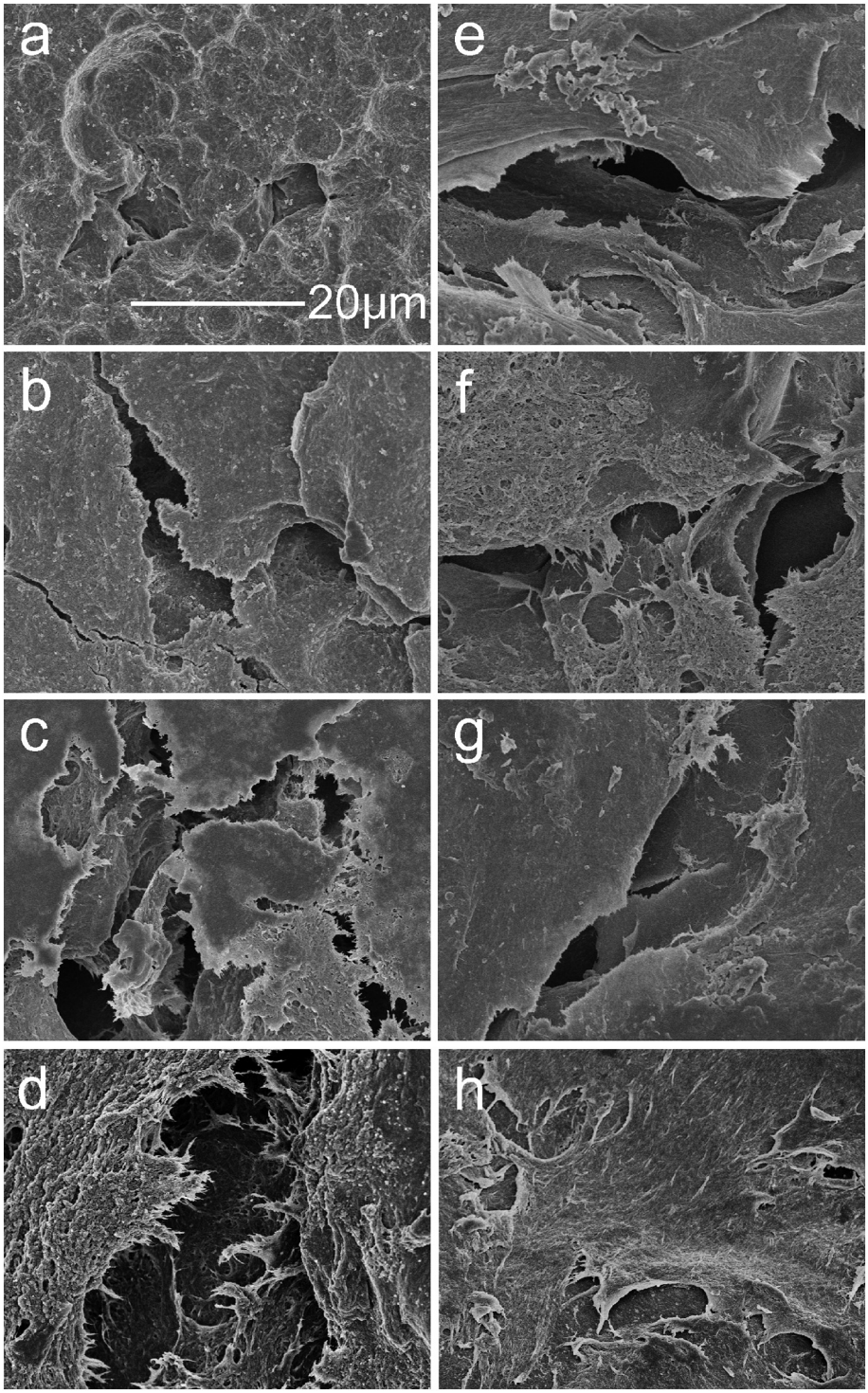

Fig. 9. SEM micrographs of degraded (a) neat PBS, (b) PBS/CT1, (c) PBS/CT5, (d) PBS/CT10, (e) PBS/CT15, (f) PBS/CT20, (g) PBS/CT25, and (h) PBS/CT30 for 4 h.

References

[1] Y.A. Chen, G.S. Tsai, E.C. Chen, T.M. Wu, J. Mater. Sci. 51 (2016) 4021–4030.
[2] J. Xu, B.H. Guo, Biotechnol. J. 5 (2010) 1149–1163.
[3] J.A. Chuah, M. Yamada, S. Taguchi, K. Sudesh, Y. Doi, K. Numata, Polym. Degrad. Stab. 98 (2013) 331–338.
[4] K.I. Kasuya, K.I. Takagi, S.I. Ishiwatari, Y. Yoshida, Y. Doi, Polym. Degrad. Stab. 59 (1998) 327–332.
[5] L. Ren, Y. Wang, J. Ge, D. Lu, Z. Liu, Macromol. Chem. Phys. 216 (2015) 636–640.
[6] M. Gigli, M. Fabbri, N. Lotti, R. Gamberini, B. Rimini, A. Munari, Eur. Polym. J. 75 (2016) 431–460.
[7] M. Fabbri, M. Gigli, R. Gamberini, N. Lotti, M. Gazzano, B. Rimini, A. Munari, Polym. Degrad. Stab. 108 (2014) 223–231.
[8] V. Siracusa, N. Lotti, A. Munari, M. Rosa, Polym. Degrad. Stab. 119 (2015) 35–45.
[9] L. Genovese, N. Lotti, M. Gazzano, V. Siracusa, M. Rosa, A. Munari, Polym. Degrad. Stab. 132 (2016) 191–201.
[10] J. Karger-Kocsis, H. Mahmood, A. Pegoretti, Prog. Mater. Sci. 73 (2015) 1–43.
[11] N. Lin, J. Yu, P.R. Chang, J. Li, J. Huang, Polym. Compos. 32 (2011) 472–482.
[12] E. Lizundia, J.L. Vilas, L.M. León, Carbohydr. Polym. 123 (2015) 256–265.
[13] X. Zhang, Y. Zhang, Carbohydr. Polym. 140 (2016) 374–382.
[14] C.N. Ludvik, G.M. Glenn, A.P. Klamczynski, D.F. Wood, J. Polym. Environ. 15 (2007) 251–257.

[15] J. Wang, M. Feng, H. Zhan, Opt. Laser Technol. 57 (2014) 84–89.
[16] X. Zhang, J. Zhu, X. Liu, Macromol. Res. 20 (2012) 703–708.
[17] X. Zhao, Y. Chen, X. Jiang, Y. Shang, L. Zhang, J. Therm. Anal. Calorim. 111 (2013) 891–896.
[18] Y. Zhao, X. Liu, J. Wang, S. Zhang, Carbohydr. Polym. 94 (2013) 723–730.
[19] Z. Yang, W. Wang, Z.Q. Shao, Cellulose 20 (2013) 159–168.
[20] H. Kang, R. Liu, Y. Huang, Polymer 70 (2015) 1–16.
[21] M.T.M. Pendergast, E.M.V. Hoek, Energy Environ. Sci. 4 (2011) 1946–1971.
[22] S. Nobukawa, H. Shimada, Y. Aoki, A. Miyagawa, V.A. Doan, Polymer 55 (2014) 3247–3253.
[23] S. Zhao, L. Zou, C.Y. Tang, D. Mulcahy, J. Membr. Sci. 396 (2012) 1–21.
[24] S. Zhang, K.Y. Wang, T.S. Chung, H. Chen, Y.C. Jean, J. Membr. Sci. 360 (2010) 522–535.
[25] T. Uesaka, N. Ogata, K. Nakane, K. Shimizu, T. Ogihara, J. Appl. Polym. Sci. 83 (2002) 1750–1758.
[26] W. Zhou, S. Yuan, Y. Chen, L. Bao, J. Appl. Polym. Sci. 124 (2012) 3124–3131.
[27] T. Uesakaa, K. Nakanea, S. Maedab, T. Ogiharaa, N. Ogataa, Polymer 41 (2000) 8449–8454.
[28] P. Číhala, O. Vopičkaa, M. Lanč, M. Kludský, J. Velas, Z. Hrdlička, A. Michalcová, M. Dendisová, K. Friess, Polym. Test. 65 (2018) 468–479.
[29] X. Hu, Z. Gao, Z. Wang, T. Su, L. Yang, Polym. Degrad. Stab. 134 (2016) 211–219.
[30] K. Nomura, Y. Nakatsuchi, R. Shinmura, J. Polym. 44 (2014) 1–4.
[31] S. Kennouch, N. Le Moigne, M. Kaci, J.C. Quantin, A.S. Caro-Bretelle, C. Delaite, J.M. Lopez-Cuesta, Eur. Polym. J. 75 (2016) 142–162.
[32] W. Luo, M. Xie, F.I. Hai, W.E. Price, D.N. Long, J. Membr. Sci. 510 (2016) 284–292.
[33] A. Cano, E. Fortunati, M. Cháfer, C. González-Martínez, A. Chiralt, J. Mater. Sci. 50 (2015) 6979–6992.
[34] T. Dong, Y. He, K. Shin, Y. Inoue, Macromol. Biosci. 4 (2004) 1084–1091.
[35] Z. Liang, P. Pan, B. Zhu, T. Dong, Y. Inoue, J. Appl. Polym. Sci. 115 (2010) 3559–3567.
[36] M. Zhou, M. Fan, Y. Zhao, T. Jin, Q. Fu, Carbohydr. Polym. 140 (2016) 383–392.
[37] L.N. Ludueña, E. Fortunati, J.I. Morán, V.A. Alvarez, V.P. Cyras, J. Appl. Polym. Sci. 133 (2016) 1–9.
[38] S. Qian, H. Mao, E. Zarei, K. Sheng, J. Polym. Environ. 23 (2015) 341–347.
[39] P. Pan, L. Zhao, J. Yang, Y. Inoue, Macromol. Mater. Eng. 298 (2013) 201–209.
[40] N.T. Leandro, F. Elena, I.M. Juan, Appl. Polym. Sci. 133 (2016) 1–9.
[41] C. Thellen, C. Orroth, D. Froio, D. Ziegler, J. Lucciarini, Polymer 46 (2005) 11716–11727.
[42] G. Tomasi, M. Scandola, B.H. Briese, D. Jendrossek, Macromolecules 29 (1996) 507–513.
[43] K. Cho, J. Lee, K. Kwon, J. Appl. Polym. Sci. 79 (2011) 1025–1033.
[44] X. Hu, T. Su, W. Pan, P. Li, Z. Wang, RSC Adv. 7 (2017) 35496–35503.
[45] S.G. Wang, B. Qiu, Polym. Adv. Technol. 4 (1993) 363–366.
[46] H. Shirahama, Y. Kawaguchi, M. S. Aludin, H. Yasuda, J. Appl. Polym. Sci. 80(2015) 340–347.